

# Controlled counter-flow motion of magnetic bead chains rolling along microchannels

Marc Karle · Johannes Wöhrle · Junichi Miwa ·  
Nils Paust · Günter Roth · Roland Zengerle ·  
Felix von Stetten

Received: 23 August 2010 / Accepted: 27 October 2010 / Published online: 10 November 2010  
© Springer-Verlag 2010

**Abstract** We demonstrate controlled transport of superparamagnetic beads in the opposite direction of a laminar flow. A permanent magnet assembles 200 nm magnetic particles into about 200  $\mu\text{m}$  long bead chains that are aligned in parallel to the magnetic field lines. Due to a magnetic field gradient, the bead chains are attracted towards the wall of a microfluidic channel. A rotation of the permanent magnet results in a rotation of the bead chains in the opposite direction to the magnet. Due to friction on the surface, the bead chains roll along the channel wall, even in counter-flow direction, up to at a maximum counter-flow velocity of  $8 \text{ mm s}^{-1}$ . Based on this approach, magnetic beads can be accurately manoeuvred within microfluidic channels. This counter-flow motion can be efficiently be used in Lab-on-a-Chip systems, e.g. for implementing washing steps in DNA purification.

**Keywords** Magnetic beads · Lab-on-a-chip · Transport · Handling

---

M. Karle (✉) · J. Wöhrle · N. Paust · G. Roth · R. Zengerle ·  
F. von Stetten  
HSG-IMIT, Wilhelm-Schickard-Strasse 10,  
78052 Villingen-Schwenningen, Germany  
e-mail: marc.karle@hsg-imit.de

J. Miwa · G. Roth · R. Zengerle · F. von Stetten  
Department of Microsystems Engineering, Laboratory  
for MEMS Applications, IMTEK, University of Freiburg,  
Georges-Köhler-Allee 106, 79110 Freiburg, Germany

G. Roth · R. Zengerle  
Centre for Biological Signalling Studies (bloss),  
University of Freiburg, Freiburg, Germany

## 1 Introduction

Recently, superparamagnetic beads have gained a lot of interest in Lab-on-a-Chip applications. The simple actuation principle with on-chip or off-chip generated magnetic fields makes magnetic beads an easy-to-handle universal tool for assay implementation (Pamme 2006).

Assays are typically implemented as sequential combinations of basic building blocks also known as microfluidic unit operations such as liquid transport, mixing, valving etc. (Haeberle and Zengerle 2007; Mark et al. 2010). Some of those unit operations have already been demonstrated using magnetic beads. Micropumps (Hatch et al. 2001; Terray et al. 2002) have been reported as well as microvalves (Terray et al. 2002; Satarkar and Hilt 2008). In hydrophobic environment, the magnetic beads can be utilised to move aqueous droplets (Egatz-Gomez et al. 2006), e.g. for nucleic acid extraction (Lehmann et al. 2006) or PCR (Ohashi et al. 2007).

With appropriate modifications on the bead surface, beads can be regarded as a moveable solid-phase carrier. This way microfluidic chips can be specifically functionalised on demand by immobilizing the beads at well-defined locations using strong magnetic fields. This approach is mainly applied for immunoassays (Furlani et al. 2007; Lacharme et al. 2008).

When exposed to an external magnetic field, the beads align and form chains along the field lines. To stabilize the chains but also add flexibility, beads covered with streptavidin can be linked via dibiotin-modified ds-DNA. Using a sinusoidal transverse field, a beating motion of the chains can be induced comparable to the motion of flagella in nature (Dreyfus et al. 2005).

By rotating the magnetic field, the beads start to rotate as well within the microfluidic chip. Rotating chains of beads

can be used for mixing (Petousis et al. 2007; Lee et al. 2009; Franke et al. 2009) and for propulsion (Tierno et al. 2008) in the vicinity of a solid surface.

Very recently, such chains of magnetic beads have been used to induce flow in microfluidic environments. The rotating external magnetic field generated a rolling motion of the bead chains close to the channel surface (Sing et al. 2010). Due to the no-slip condition at the surface, the bead chains caused the surrounding fluid to flow in a predefined direction. This surface-induced flow was used to transport vesicles.

In this article, we demonstrate that this rolling motion can be used for controlled movement of the magnetic beads within a microfluidic channel (Fig. 1). In comparison to other approaches with electromagnets on planar glass surfaces with magnetic films and in the absence of fluidic flow (Morimoto et al. 2008), we use a single rotating permanent magnet to generate the rotating magnetic field. Furthermore, this single magnet at the same time provides the field gradient required to attract the beads towards the channel wall.

## 2 Materials and methods

### 2.1 Chip production

The structure of the microfluidic channel was designed with CAD software. The standard channel dimensions were set to a depth of 210  $\mu\text{m}$  and a width of 300  $\mu\text{m}$ . Using a 300  $\mu\text{m}$  milling head (F126.0030, GIS Gienger Industrie-Service, Zurich, Switzerland) together with a precision

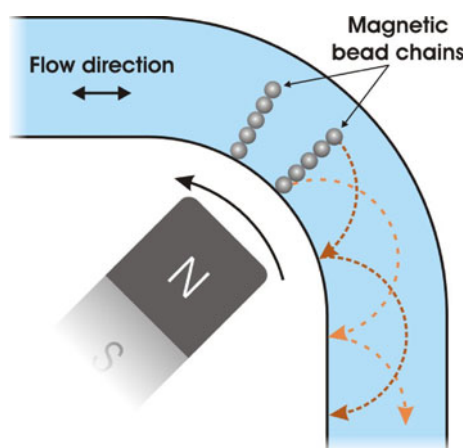


**Fig. 1** Schematic of the experimental set-up. A rotating permanent magnet attracts the magnetic beads towards the inner channel wall. The movement of the magnetic beads is observed in a section of the microfluidic channel that is circularly arranged around the permanent magnet. The bead chains roll along the microchannel

milling machine (Minitech Machinery Corporation, Norcross, Georgia 30092, USA) the microfluidic channels were milled into a polycarbonate substrate (blank DVD, Sonopress GmbH, Gütersloh, Germany). After cleaning with DI water as well as isopropanol and drying with nitrogen the chip was sealed with adhesive foil (676070, Greiner Bio-One GmbH, Frickenhausen, Germany).

### 2.2 Fluidic set-up

The superparamagnetic beads with a diameter of 200 nm were taken from a commercially available DNA extraction kit (ajInnuscreen, Berlin, Germany). The stock solution of magnetic beads was diluted 200-fold to 0.5% in elution buffer provided with the kit. This dilution was chosen since it offers the best conditions for observing and analysing the movement of the bead chains: As only very few bead chains form at lower concentrations, the time between bead chains passing the observation window increases whereas at higher densities too many chains populating the observation window prevent the analysis of the movement of individual chains.

The magnetic beads were filled into glass syringes (1001 TLL, Hamilton, Bonaduz, Switzerland) and injected into the chip using a precision syringe pump (neMESYS, Cetoni, Korbußen, Germany) for defined constant flow rates.

### 2.3 Generating the rotating magnetic field

A NdFeB permanent magnet (Q-19-13-06-LN,  $19.1 \times 12.7 \times 6.4 \text{ mm}^3$ , Webcraft, Uster, Switzerland) was used to actuate the magnetic beads. The magnet was mounted onto a stepper motor (Nanotec, Landsham, Germany) to generate rotary motion of the magnet and thus a rotating magnetic field. With a computer programme written in Visual Basic a TMC3200 stepper motor controller (Trinamic, Hamburg, Germany) defined the rotational frequency of the permanent magnet. The magnet was positioned directly underneath the microfluidic chip so that the distance from its tip to the inner channel wall was 5 mm throughout the test section. The magnetic flux density at this distance from the tip of the magnet is

$$\vec{B} = 43 \text{ mT}$$

with a gradient of

$$|\nabla B| = 11.6 \frac{\text{T}}{\text{m}}.$$

### 2.4 Measurement of bead movement

The movement of the magnetic bead chains has been recorded with a high speed camera (pco.1200s b/w, PCO AG, Kehlheim, Germany). The video clips were then

analyzed for bead chain velocity inside the microfluidic channels.

If the magnetic beads are diluted enough to form single bead chains within the microfluidic channels then they can be tracked easily throughout consecutive frames of the video clip. The change in location together with the frame rate yields the velocity of the magnetic bead chains.

### 3 Results and discussion

Under the influence of the strong magnetic field of the off-chip permanent magnet, the magnetic beads align along the field lines and form flagella-like chains (Fig. 2). When rotating the permanent magnet the magnetic field rotates as well. At the location of the bead chains this causes the field lines to turn. The bead chains follow the field lines and accordingly also start to rotate.

Due to the field gradient of the permanent magnet, the magnetic bead chains are attracted towards the inner channel wall facing the magnet. The microfluidic channel is designed circularly along the magnet tip trajectory to ensure that the magnetic force vector always points perpendicularly to the channel wall (towards the centre).

In consequence of the magnet rotation, the bead chains roll on the channel wall. As they are trapped on their supporting point at the channel wall the magnetic bead chains ‘walk’ along the channel wall (Figs. 2, 3a).

To determine the velocity of the magnetic beads inside the microfluidic channels, four individual bead chains were

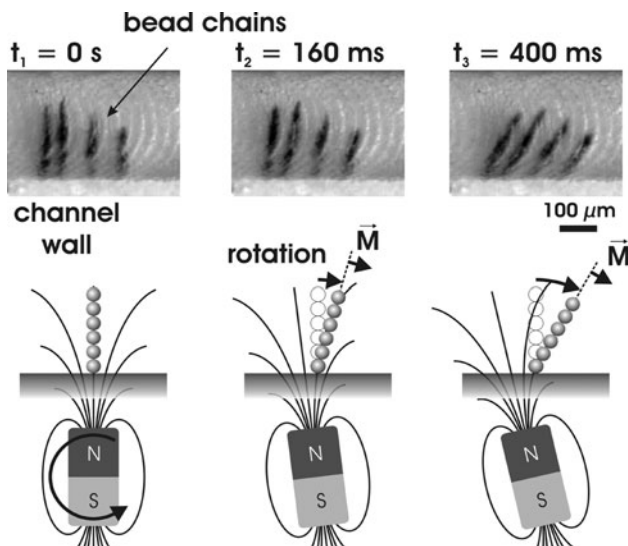


**Fig. 2** Illustration of the magnetic bead chain movement in a periodically varying magnetic field induced by a rotating permanent magnet ( $f = 0.25$  Hz). The magnetic beads align to form flagella-like chains along the magnetic field lines. As the magnetic field rotates, the chains follow the magnetic field lines due to a torque  $\vec{M}$  resulting in a rotation in the opposite direction

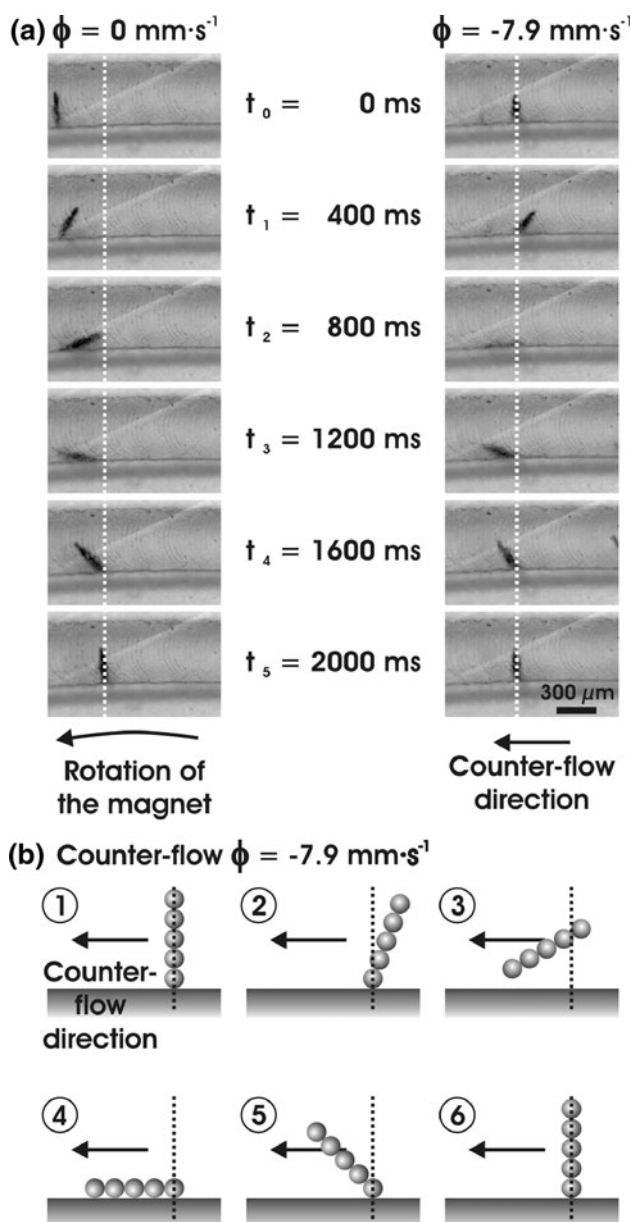


**Fig. 3** **a** Instantaneous images of the bead movement. Rotational frequency of the magnet was set to 0.25 Hz. *Left* When no flow is applied the bead chains move along the channel wall. The step size (distance moved in one 180° turn) corresponds to the length of the bead chain. *Right* At a counter-flow velocity of  $-7.9 \text{ mm s}^{-1}$  the beads remain at their position. **b** Schematic illustration of the bead movement at counter-flow conditions. During the phase depicted in (3) the bead chain detaches from the channel wall

tracked for each fluid flow condition over the time period of two complete rotations. The beads were tracked with no flow applied as well as under several co-flow and counter-flow conditions and different rotational frequencies of the permanent magnet. The bead chain velocity depends on the length of the chains since long chains move over a larger distance per cycle compared to short chains. Therefore, only bead chains of about 200 μm in length have been

selected for the evaluation out of a population containing chains ranging from 50 to 300  $\mu\text{m}$ .

Data depicted in Fig. 4 clearly indicate a linear relationship between the rotational frequency of the permanent magnet and the velocity of the bead chains. When doubling the rotational frequency, the beads move twice as fast. This result can be explained as the bead chains rotate with the same frequency as the magnet. Therefore, at higher frequencies they perform more steps per time interval and thus move faster.

Even at rotational frequencies up to 10 Hz of the magnet and thus the magnetic field, the bead chains follow the field lines rotating at the same rotational frequency. Interestingly, in contrast to Sing et al. (2010) we did not observe a break-up of the bead chains. This might be due to the difference in nature of the beads chains: Sing et al. (2010) uses chains comprising only few individual beads. Our chains on the other hand consist of several thousand of beads agglomerated to a large chain.

Furthermore, the bead chain velocity also depends on the applied flow rate. In this case, the movement of the beads is not only generated by friction on the channel wall but also by fluidic drag. The bead chains move faster when the magnetically induced motion and the fluid flow are parallel. When the two acting forces are opposing each other the beads slow down at low counter-flow rates until they remain at their location for a mean flow velocity of about  $\phi = -8.0 \text{ mm s}^{-1}$ , corresponding to a flow rate of  $-0.5 \mu\text{l s}^{-1}$  (Fig. 3a). For higher counterflow velocities,

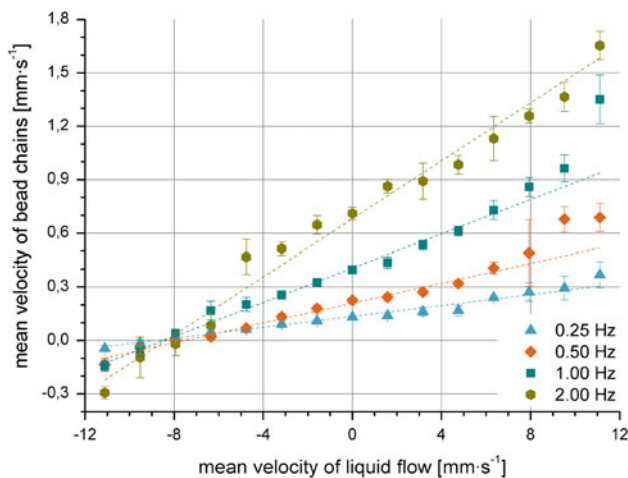


**Fig. 4** Mean velocity of the bead chains versus mean velocity of the applied flow at different rotational frequencies of the permanent magnet. Each point represents the mean value of four independent bead chains of about 200  $\mu\text{m}$  in length that have been tracked for two complete rotations (*error bars* indicate the standard deviation). The mean bead velocity depends linearly on the rotational frequency of the magnet. Under the experimental conditions, the bead chains could withstand and even move against a counter-flow velocity of up to  $-8.0 \text{ mm s}^{-1}$  irrespective of the velocity of the magnet

the beads are dragged downstream with the flow. Consequently, for flow velocities in the range of  $-8.0 < \phi < 0 \text{ mm s}^{-1}$  the magnetic beads can be manoeuvred in the opposite direction to the fluid flow.

The transport of the magnetic beads by fluid flow is schematically depicted in Fig. 3b. Usually, the bead chains are carried away when they are inclined against the flow direction (see Fig. 3a right between 400 and 800 ms) as the fluidic drag lowers the traction at the supporting point. The chains detach from the wall and continue to rotate. As soon as they are oriented parallel to the flow direction, the shear-induced lift force vanishes, and the magnetic force causes the chain to re-attach to the channel wall. Primarily, whilst the bead chains are detached, they are carried downstream by the fluid flow because of the lack of any friction force. Only very rarely they are shifted in position during other phases of the rotational movement.

A quantitative analysis of the involved forces is beyond the scope of this article since the complex interaction of fluidic drag and magnetic force change dynamically with the rotation of the bead chains.

Although the laminar flow profile is nonlinear (parabolic), the total force or the torque acting on the bead chains should scale linearly with varying mean velocity. The linear fits in Fig. 4 support a linear relationship between the bead velocity and the applied flow velocity (with an offset of  $-8.0 \text{ mm s}^{-1}$ ). Hence, the parabolic flow profile seems to have no influence on the movement of the bead chains. The bead velocity is, therefore, determined by only two parameters; the rotational frequency of the magnetic field and the mean velocity of the surrounding fluid in which the magnetic beads are suspended.

The roughness of the channel walls resulting from the milling process is mainly responsible for the deviation from the mean values in bead chain motion. As the surface roughness directly influences the friction between the magnetic beads and the channel wall, error bars grow with the fluid velocity.

## 4 Conclusions

In this study, we presented a simple approach for controlled transport of superparamagnetic beads inside microfluidic channels. A rotating magnetic field generated by a rotating permanent magnet induces the rotation of magnetic bead chains which ‘walk’ along the walls of microfluidic channels. This was possible even for a counter-flow arrangement with a mean liquid velocity of up to  $-8.0 \text{ mm s}^{-1}$ . The use of this method within a real world biological assay implementation such as continuous DNA extraction has been shown in (Karle et al. 2010). Furthermore, the walking bead chains enable a wide range of other

applications from transport to positioning of the target molecules or cells.

**Acknowledgments** This study is funded by the German Federal Ministry of Education and Research (16SV3528).

## References

- Dreyfus R, Baudry J, Roper ML, Fermigier M, Stone HA, Bibette J (2005) Microscopic artificial swimmers. *Nature* 437(7060): 862–865
- Egatz-Gomez A, Melle S, Garcia AA, Lindsay SA, Marquez M, Dominguez-Garcia P, Rubio MA, Picraux ST, Taraci JL, Clement T, Yang D, Hayes MA, Gust D (2006) Discrete magnetic microfluidics. *Appl Phys Lett* 89(3):034106
- Franke T, Schmid L, Weitz DA, Wixforth A (2009) Magneto-mechanical mixing and manipulation of picoliter volumes in vesicles. *Lab Chip* 9(19):2831–2835
- Furlani EP, Sahoo Y, Ng KC, Wortman JC, Monk TE (2007) A model for predicting magnetic particle capture in a microfluidic bioseparator. *Biomed Microdevices* 9(4):451–463
- Haeberle S, Zengerle R (2007) Microfluidic platforms for lab-on-a-chip applications. *Lab Chip* 7(9):1094–1110
- Hatch A, Kamholz AE, Holman G, Yager P, Bohringer KF (2001) A ferrofluidic magnetic micropump. *J Microelectromech Syst* 10(2): 215–221
- Karle M, Miwa J, Czilwik G, Auwärter V, Roth G, Zengerle R, von Stetten F (2010) Continuous microfluidic DNA extraction using phase-transfer magnetophoresis. *Lab Chip*. doi: [10.1039/C0LC00129E](https://doi.org/10.1039/C0LC00129E)
- Lacharme F, Vandevyver C, Gijs MAM (2008) Full on-chip nanoliter immunoassay by geometrical magnetic trapping of nanoparticle chains. *Anal Chem* 80(8):2905–2910
- Lee SH, van Noort D, Lee JY, Zhang BT, Park TH (2009) Effective mixing in a microfluidic chip using magnetic particles. *Lab Chip* 9(3):479–482
- Lehmann U, Vandevyver C, Parashar VK, Gijs MAM (2006) Droplet-based DNA purification in a magnetic lab-on-a-chip. *Angew Chem Int Ed* 45(19):3062–3067
- Mark D, Haeberle S, Roth G, von Stetten F, Zengerle R (2010) Microfluidic lab-on-a-chip platforms: requirements, characteristics and applications. *Chem Soc Rev* 39:1153–1182
- Morimoto H, Ukai T, Nagaoka Y, Grobert N, Maekawa T (2008) Tumbling motion of magnetic particles on a magnetic substrate induced by a rotational magnetic field. *Phys Rev E* 78(2):021403
- Ohashi T, Kuyama H, Hanafusa N, Togawa Y (2007) A simple device using magnetic transportation for droplet-based PCR. *Biomed Microdevices* 9(5):695–702
- Pamme N (2006) Magnetism and microfluidics. *Lab Chip* 6(1):24–38
- Petousis I, Homburg E, Derks R, Dietzel A (2007) Transient behaviour of magnetic micro-bead chains rotating in a fluid by external fields. *Lab Chip* 7(12):1746–1751
- Satarkar NS, Hilt JZ (2008) Magnetic hydrogel nanocomposites for remote controlled pulsatile drug release. *J Control Release* 130(3): 246–251
- Sing CE, Schmid L, Schneider MF, Franke T, Alexander-Katz A (2010) Controlled surface-induced flows from the motion of self-assembled colloidal walkers. *Proc Natl Acad Sci USA* 107(2): 535–540
- Terray A, Oakey J, Marr DWM (2002) Microfluidic control using colloidal devices. *Science* 296(5574):1841–1844
- Tierno P, Golestanian R, Pagonabarraga I, Sagues F (2008) Controlled swimming in confined fluids of magnetically actuated colloidal rotors. *Phys Rev Lett* 101(21):218–304